Supplement of Atmos. Chem. Phys., 17, 3253–3278, 2017
http://www.atmos-chem-phys.net/17/3253/2017/
doi:10.5194/acp-17-3253-2017-supplement
© Author(s) 2017. CC Attribution 3.0 License.

Atmospheric Chemistry and Physics
Open Access

Supplement of

Sensitivity of the interannual variability of mineral aerosol simulations to meteorological forcing dataset

Molly B. Smith et al.

Correspondence to: Molly B. Smith (mbsmith@albany.edu)

The copyright of individual parts of the supplement might differ from the CC-BY 3.0 licence.

Table S1: Variability (defined as the standard deviation over the mean) at each station for the annual mean concentration for 1990-2005 (a) and AOD (b) from the model and observations for each station (Figure 1 and 2). Variability from the observations is also shown.

a. Surf. Conc.	Banizoumbou	Barbados	Bermuda	Cinzana	Izana	Mace-head	Mbour	Miami	Midway
CAM4 (MERRA)	0.13	0.27	0.39	0.08	0.28	0.51	0.10	0.34	0.31
CAM4 (NCEP)	0.21	0.27	0.32	0.13	0.30	0.62	0.12	0.34	0.28
CAM4 (ERAI)	0.10	0.13	0.27	0.09	0.28	0.28	0.06	0.19	0.21
CAM4 (AMIP)	0.13	0.13	0.20	0.09	0.19	0.37	0.06	0.19	0.18
GCHEM (MERRA)	0.21	0.28	0.38	0.21	0.34	0.34	0.23	0.39	0.25
MATCH (NCEP)	0.25	0.22	0.38	0.16	0.32	0.60	0.15	0.35	0.29
CAM5 (AMIP)	0.14	0.24	0.28	0.14	0.32	0.78	0.21	0.36	0.27
Obs.	0.27	0.20	0.56	0.22	0.33	0.44	0.35	0.36	0.40

b. AOD	Bahrain	Dalanzadgad	Ilorin	Sede Boker
CAM4 (MERRA)	0.06	0.11	0.16	0.17
CAM4 (NCEP)	0.10	0.14	0.17	0.20
CAM4 (ERAI)	0.09	0.17	0.12	0.14
CAM4 (AMIP)	0.10	0.11	0.16	0.14
GCHEM (MERRA)	0.50	0.75	0.95	0.86
MATCH (NCEP)	0.48	0.62	0.84	0.80
CAM5 (AMIP)	0.70	0.83	0.82	0.62
Obs.	0.24	0.17	0.42	0.06

Table S2: Variability (defined as the standard deviation over the mean) at each station for the seasonal cycle (climatological monthly mean of 12 months) concentration for 1990-2005 (a) and AOD (b) from the model and observations for each station (Figure S1 and S3). Variability from the observations is also shown.

a. Surf. Conc.	Banizoumbou	Barbados	Bermuda	Cinzana	Izana	Mace-head	Mbour	Miami	Midway
CAM4 (MERRA)	0.66	0.57	1.11	0.69	1.20	0.78	0.33	1.36	1.21
CAM4 (NCEP)	0.64	0.80	1.26	0.76	1.09	0.81	0.34	1.50	1.28
CAM4 (ERAI)	0.48	0.69	0.84	0.50	1.11	0.51	0.37	1.06	0.73
CAM4 (AMIP)	0.70	0.17	0.78	0.51	0.64	0.23	0.40	0.83	0.73
GCHEM(MERRA)	0.77	0.53	1.06	0.59	1.03	0.73	0.83	1.13	0.96
MATCH (NCEP)	0.77	0.57	1.37	0.71	1.06	1.15	0.64	1.33	0.85
CAM5 (AMIP)	0.72	0.72	1.25	0.60	0.79	0.96	0.70	1.32	0.88
Obs.	0.65	0.56	1.41	0.65	0.55	0.72	0.51	1.09	1.40

b. AOD	Bahrain	Dalanzadgad	Ilorin	Sede Boker
CAM4 (MERRA)	0.47	0.56	0.42	0.42
CAM4 (NCEP)	0.48	0.71	0.33	0.50
CAM4 (ERAI)	0.43	0.50	0.31	0.43
CAM4 (AMIP)	0.53	0.61	0.53	0.69
GCHEM (MERRA)	0.45	0.75	0.81	0.71
MATCH (NCEP)	0.38	0.54	0.68	0.63
CAM5 (AMIP)	0.68	0.74	0.70	0.38
Obs.	0.27	0.42	0.52	0.22

Table S3: Correlation of annual mean concentration between model and observed values for each case and station for 1990-2005 for concentrations (a) and AOD (b). Correlations which are statistically significant at the 95 percentile level are in bold. Note that only the stations with overlapping time periods with the model runs with multiple years are included in this analysis. CAM4-Re is the mean time series from the CAM4 (MERRA), CAM4 (NCEP) and CAM4 (ERAI) model simulations.

a. Surf. Conc.	Barbados	Bermuda	Izana	Mace Head	Miami	Midway
CAM4 (MERRA)	0.16	0.64	0.08	0.26	-0.25	-0.72
CAM4 (NCEP)	0.15	**0.78**	0.33	0.63	-0.17	-0.66
CAM4 (ERAI)	0.19	0.14	0.28	0.66	0.37	-0.79
CAM4 (AMIP)	0.21	-.011	0.12	-0.62	-0.20	-0.33
GCHEM (MERRA)	0.16	0.36	0.28	-0.27	-0.20	-0.53
MATCH (NCEP)	0.14	**0.92**	0.31	0.23	-0.20	-0.73
CAM5 (AMIP)	0.23	0.14	0.06	-0.08	-0.34	-0.37
CAM4-RE	0.20	0.43	0.21		-0.02	-0.71

b. AOD	Bahrain	Dalanzad gad	Ilorin	Sede Boker
CAM4 (MERRA)	-0.12	0.55	0.47	-0.35
CAM4 (NCEP)	0.22	0.37	0.60	-0.36
CAM4 (ERAI)	-0.32	0.10	0.28	-0.39
CAM4 (AMIP)	0.12	-0.12	-0.78	-0.59
GCHEM(MERRA)	-0.73	0.25	**0.78**	-0.23
MATCH (NCEP)	0.23	0.51	0.56	-0.12
CAM5 (AMIP)	0.10	-0.09	0.63	0.33
CAM4-RE	-0.11	0.48	0.47	-0.37

Table S4: Correlation of mean seasonal cycle (12 climatological monthly means) between model and observed values for each case and station for 1990-2005 for concentrations (Figure S7) (a) and AOD (Figure S8) (b). Correlations which are statistically significant at the 95 percentile level are in bold. Note that only the stations with overlapping time periods with the model runs are included in this analysis. CAM4-RE is the average of the model CAM4 (MERRA), CAM4 (NCEP) and CAM4(ERAI).

a. Surf. Conc.	Barbados	Bermuda	Izana	Mace Head	Miami	Midway
CAM4 (MERRA)	**0.90**	**0.98**	-0.49	0.30	**0.98**	**0.96**
CAM4 (NCEP)	**0.98**	**0.97**	-0.45	0.39	**0.99**	**0.83**
CAM4 (ERAI)	**0.95**	**0.96**	-0.46	0.42	**0.98**	**0.90**
CAM4 (AMIP)	0.15	**0.78**	-0.54	0.29	**0.77**	**0.28**
GCHEM (MERRA)	**0.83**	**0.95**	-0.39	0.55	**0.94**	**0.95**
MATCH (NCEP)	**0.87**	**0.95**	-0.41	0.48	**0.97**	**0.88**
CAM5 (AMIP)	**0.79**	**0.95**	-0.46	**0.61**	**0.95**	**0.56**
CAM4 (RE)	**0.94**	**0.97**	-0.46	0.38	**0.98**	**0.92**

b. AOD	Bahrain	Dalanzadgad	Ilorin	Sede Boker
CAM4 (MERRA)	**0.89**	**0.80**	**0.83**	0.20
CAM4 (NCEP)	**0.84**	**0.70**	**0.89**	0.38
CAM4 (ERAI)	**0.77**	**0.95**	**0.75**	0.35
CAM4 (AMIP)	**0.82**	**0.70**	**0.91**	0.40
GCHEM (MERRA)	**0.84**	**0.89**	**0.98**	0.21
MATCH (NCEP)	**0.55**	**0.61**	**0.96**	0.33
CAM5 (AMIP)	**0.71**	**0.82**	**0.94**	0.41
CAM4 (RE)	**0.86**	**0.82**	**0.84**	0.31

Table S5: Meteorological drivers of CAM4 model results in the Western Sahel and North Africa. Correlation between IAV in mobilization (source) and different meteorological variables (statistically significant values at 95% bold face), in the Western Sahel (13 to 22°N and -20 to 13°E). Only gridboxes which are active in each model are included in the calculation for that model.

	Precip.	Soil moisture	LAI	Sfc. Wind
CAM4 (MERRA)	**-0.20**	**-0.21**	**-0.20**	**0.78**
CAM4 (NCEP)	**-0.50**	**-0.47**	**-0.62**	**0.87**
CAM4 (ERAI)	-0.15	-0.16	**-0.41**	**0.63**
CAM4 (AMIP)	-0.13	-0.12	-0.15	**0.94**

Table S6: Meteorological drivers of CAM4 model results in the Western Sahel region (13 to 22°N and -20 to 13°E). Slope of the normalized annual mean values from 1982 to 2008 (or time period available, shown in Table 1) for each region and model (statistically significant values are in bold). Values are normalized by dividing by the mean, so that slopes represent relative change per year. Only gridboxes which are active in each model are included in the calculation for that model.

	Precip.	Soil moisture	LAI	Sfc. Wind
CAM4 (MERRA)	0.0005	-0.001	**-0.0073**	**-0.0036**
CAM4 (NCEP)	**0.0443**	**0.016**	**0.057**	**-0.0036**
CAM4 (ERAI)	0.0010	**-0.0027**	-0.0001	**-0.0007**
CAM4 (AMIP)	**0.0194**	**0.0079**	**0.015**	**-0.0016**

Table S7: Correlation of variables for South American (Argentinian) dust sources in different model versions (statistically significant values at 95% bold face). The values are the correlation across time series averaged over the grid-boxes which are active sources in each model (which is different between different versions).

	Precip.	Soil moisture	LAI	Sfc. Wind
CAM4 (MERRA)	-0.04	0.04	**-0.56**	**-0.27**
CAM4 (NCEP)	**0.31**	**0.49**	**-0.63**	**-0.51**
CAM4 (ERAI)	**0.23**	**0.29**	**-0.33**	**-0.22**
CAM4 (AMIP)	-0.06	0.04	**-0.47**	**0.45**

Table S8: Slopes in mobilization and meteorological variables in different regions for the annual average over 1990-2005 in each region (only including gridboxes which are active at any time in that model simulation). Values shown are the averages of the slopes across the CAM4-Reanalysis models (CAM4(MERRA), CAM4(NCEP) and CAM4(ERAI)). The regions are defined as in Table 6. Bold values represent slopes that are larger than the average across the models of the one sigma error in the regression.

	Source.	Precipitation	Leaf Area Index	Sfc. Wind
Australia	**0.051**	-0.013	**-0.032**	**-0.0026**
East Asia	-0.0035	**0.006**	-0.0025	-0.0011
Middle East	-0.0012	-0.0022	0.0066	0.0001
North Africa	-0.0003	-0.0015	0.0024	**-0.0018**
North America	0.0024	-0.0069	**-0.0172**	-0.0001
Sahel (Western)	**-0.0087**	**0.0135**	**0.0239**	**-0.0039**
South Africa	**-0.011**	**0.0243**	**0.0392**	0.0012
South America (Argentina)	**-0.13**	0.001	0.0107	0.0016
Globe	-0.0005	0.0012	**0.0035**	**-0.0011**

Table S9: Deposition into ocean basins. For each ocean region, the averaged correlation across time between annual mean deposition fluxes for the CAM-RE cases is shown in the second column. The following columns show the climatological mean deposition flux (Tg/year) for each model simulation. Regions are defined as the ocean gridboxes (not

including sea ice or land boxes) in the following latitude and longitude areas as from (Gregg et al., 2003): North Atlantic (>30°N; 270 to 30°E); North Pacific (>30°N; 120 to 270°E); North Central Atlantic (10 to 30°N, 270 to 30°E); North Central Pacific (10 to 30N; 120 to 270°E); North Indian (10 to 30°N; 30 to 120°E); Equatorial Atlantic (-10 to 10°N; 300 to 30°E); Equatorial Pacific (-10 to 10°N; 120 to 285°E); Equatorial Indian (-10 to 10°N; 30-120°E); South Atlantic (-30 to -10°N; 30 to 300°E); South Pacific (-30 to -10°N; 120 to 295°E); South Indian (-30 to -30°N, 30 to 120°E); Antarctic (<-30°N).

	Correlation	Mean CAM4-Re	Mean all
North Atlantic	0.68	54 +/-7%	61 +/-17%
North Pacific	0.50	30 +/- 30%	30 +/- 60%
North Central Atlantic	0.66	91 +/- 8%	120 +/- 30%
North Central Pacific	0.33	20 +/- 90%	20 +/- 90%
North Indian	0.10	100 +/- 30%	110 +/- 40%
Equatorial Atlantic	0.39	77 +/- 20%	80 +/- 35%
Equatorial Pacific	0.33	4 +/- 100%	6 +/- 130%
Equatorial Indian	0.31	23 +/- 25%	21 +/-23%
South Atlantic	0.16	3+/-60%	3 +/- 90%
South Pacific	0.62	1 +/- 40%	3 +/- 60%
South Indian	0.38	2 +/- 40%	4 +/- 75%
Antarctic	0.35	15 +/- 100%	30 +/- 100%
Global	0.45	450 +/- 10%	510 +/- 24%

Table S10: AOD for each ocean basin. For each ocean region, the averaged correlation across time between annual mean AOD for the CAM-RE cases is shown in the second column. The following columns show the climatological mean AOD for each model simulation. Regions are defined as the ocean gridboxes (not including sea ice or land boxes) in the following latitude and longitude areas as from (Gregg et al., 2003): North Atlantic (>30°N; 270 to 30°E); North Pacific (>30°N; 120 to 270°E); North Central Atlantic (10 to 30°N, 270 to 30°E); North Central Pacific (10 to 30N; 120 to 270°E); North Indian (10 to 30°N; 30 to 120°E); Equatorial Atlantic (-10 to 10°N; 300 to 30°E); Equatorial Pacific (-10 to 10°N; 120 to 285°E); Equatorial Indian (-10 to 10°N; 30-120°E); South Atlantic (-30 to -10°N; 30 to 300°E); South Pacific (-30 to -10°N; 120 to 295°E); South Indian (-30 to -30°N, 30 to 120°E); Antarctic (<-30°N).

	Correlation	Mean CAM4-Re	Mean all
North Atlantic	0.29	0.019+/-60%	0.021 +/-60%
North Pacific	0.42	0.013+/-50%	0.014 +/- 80%
North Central Atlantic	0.52	0.060 +/- 40%	0.075 +/- 60%
North Central Pacific	0.01	0.008 +/- 100%	0.010 +/- 120%
North Indian	0.58	0.087 +/- 20%	0.070 +/- 30%
Equatorial Atlantic	0.34	0.066 +/- 50%	0.055 +/- 70%
Equatorial Pacific	0.12	0.001 +/- 130%	0.002 +/- 170%
Equatorial Indian	0.54	0.012 +/- 40%	0.009 +/- 60%
South Atlantic	0.59	0.004 +/- 50%	0.003 +/-60%

South Pacific	0.69	0.001 +/- 70%	0.001 +/- 50%
South Indian	0.59	0.002 +/- 50%	0.002 +/- 40%
Antarctic	0.33	0.001 +/- 100%	0.001 +/- 60%
Global	0.43	0.012+/-50%	0.012 +/- 60%

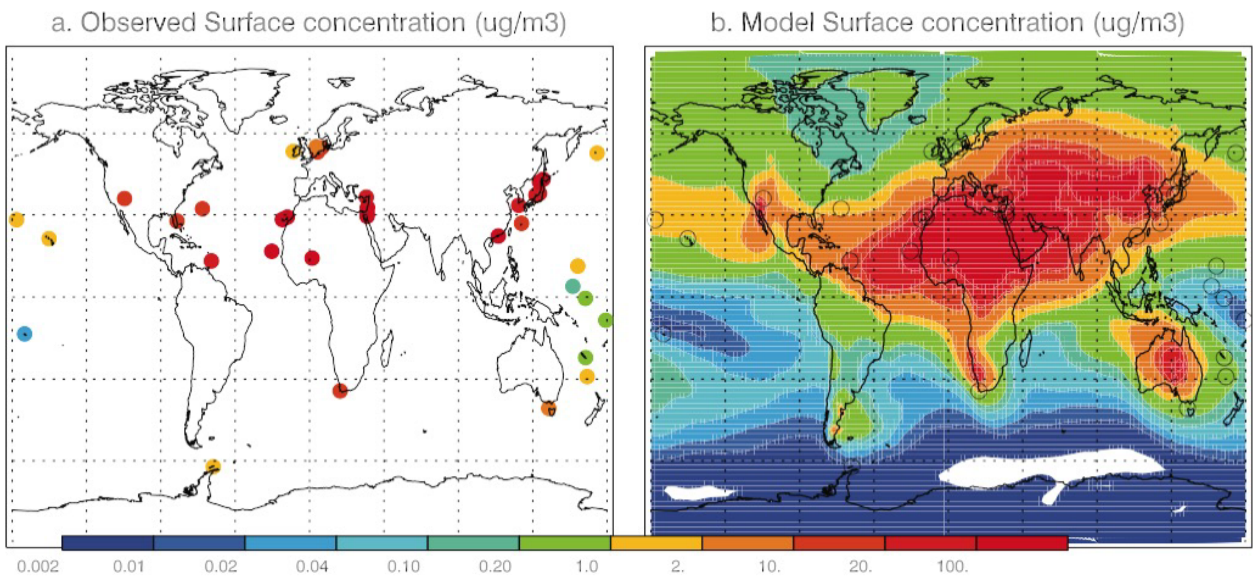

Figure S1: Spatial plot of the observed annually average distribution of dust concentrations for observations from (Albani et al., 2014) (a) and model simulation using CAM4 (MERRA) case in µg/m^3 (b). Observational sites used in the correlation coefficient comparison to shown with circles, while the 'x' mark the long-term stations used for IAV evaluation.

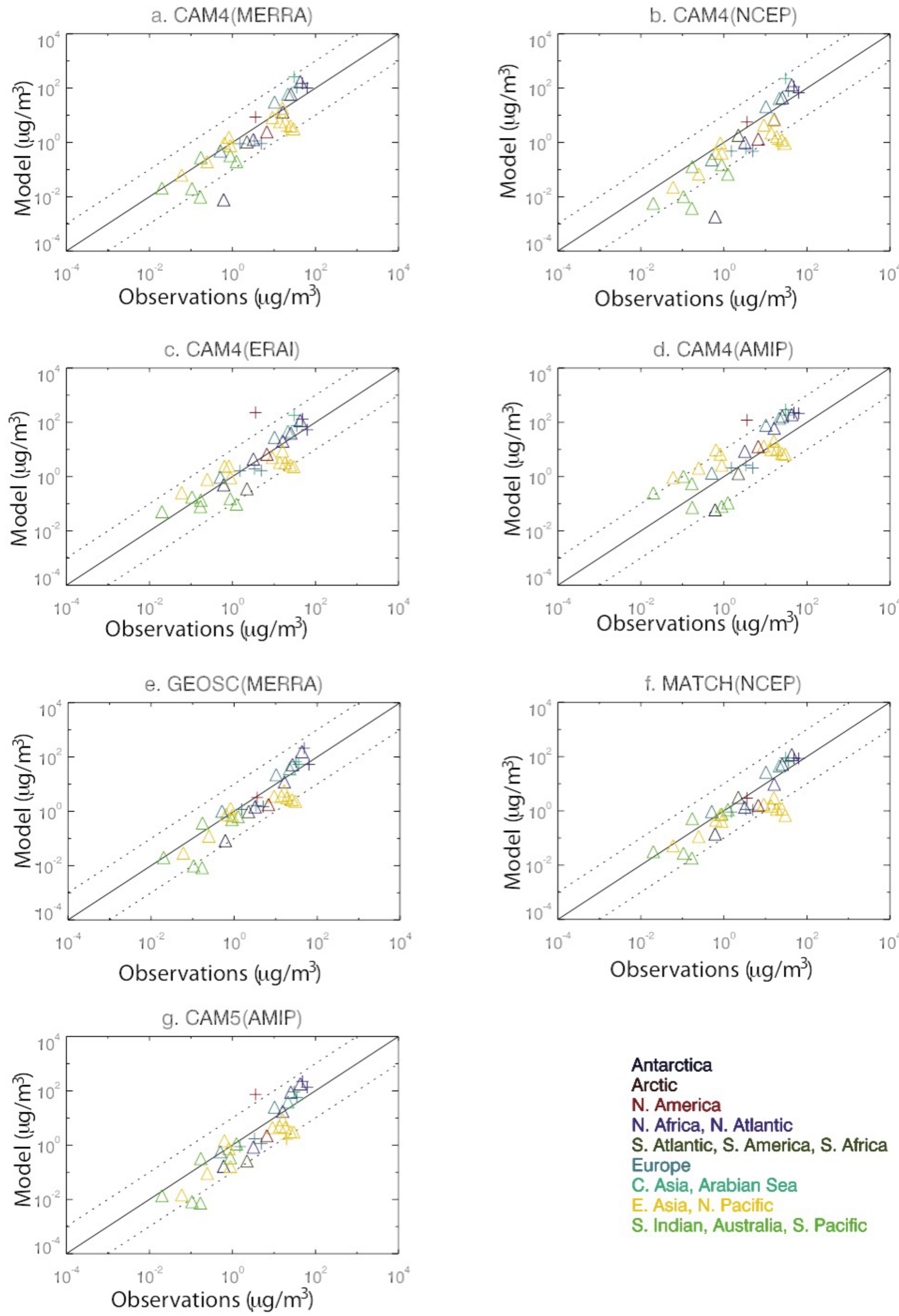

Figure S2: Scatterplot of annually averaged concentration measurements (μg/m^3) as shown in Figure S1 versus model results for the cases considered here: CAM4 (MERRA) (a), CAM4 (NCEP) (b), CAM4 (ERAI) (c), CAM4 (AMIP) (d), GEOSC (MERRA) (e), MATCH (NCEP) (f), CAM5 (AMIP) (g). Cases described in Table 1, correlation coefficients for these comparisons are shown in Table 2. Crosses are University of Miami sites (e.g. (Prospero, 1990; Prospero, 1996)); triangles are sites from (Mahowald et al., 2009). Colors indicate broad regions as in legend.

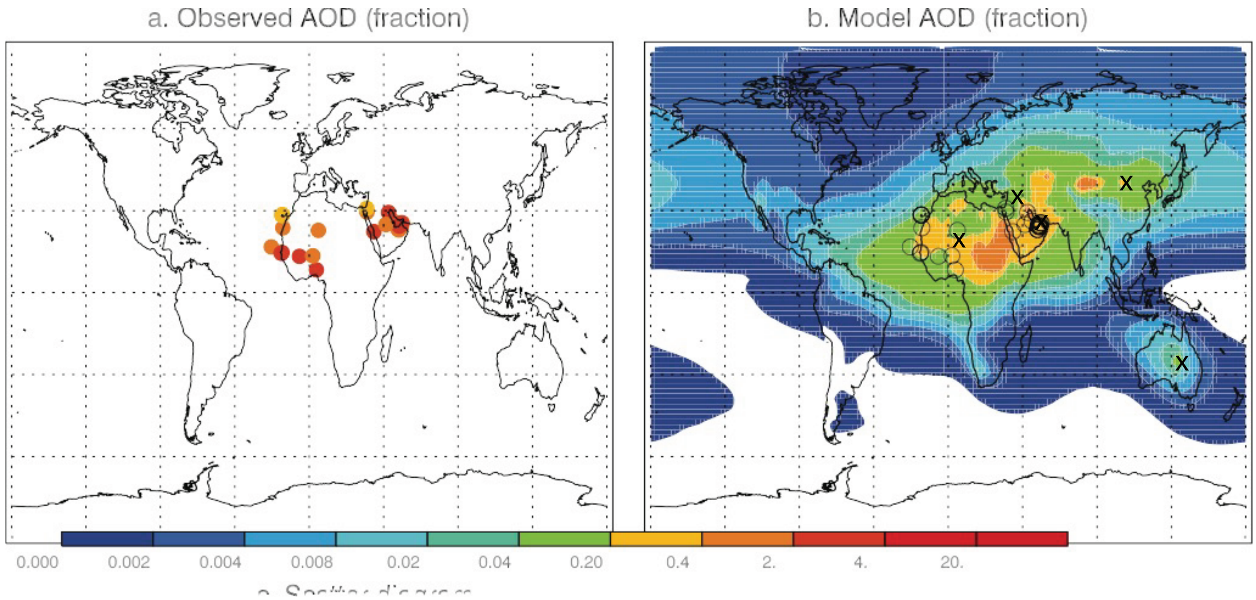

Figure S3: Spatial plot of the observed annually averaged AOD for AERONET observations (Holben *et al.*, 2001) in dust dominated regions (a) and model simulation using CAM4 (MERRA) case (b). Observational synthesis from (Albani *et al.*, 2014). Observational sites used in the correlation coefficient comparison to shown with circles, while the 'x' mark the long-term stations used for IAV evaluation.

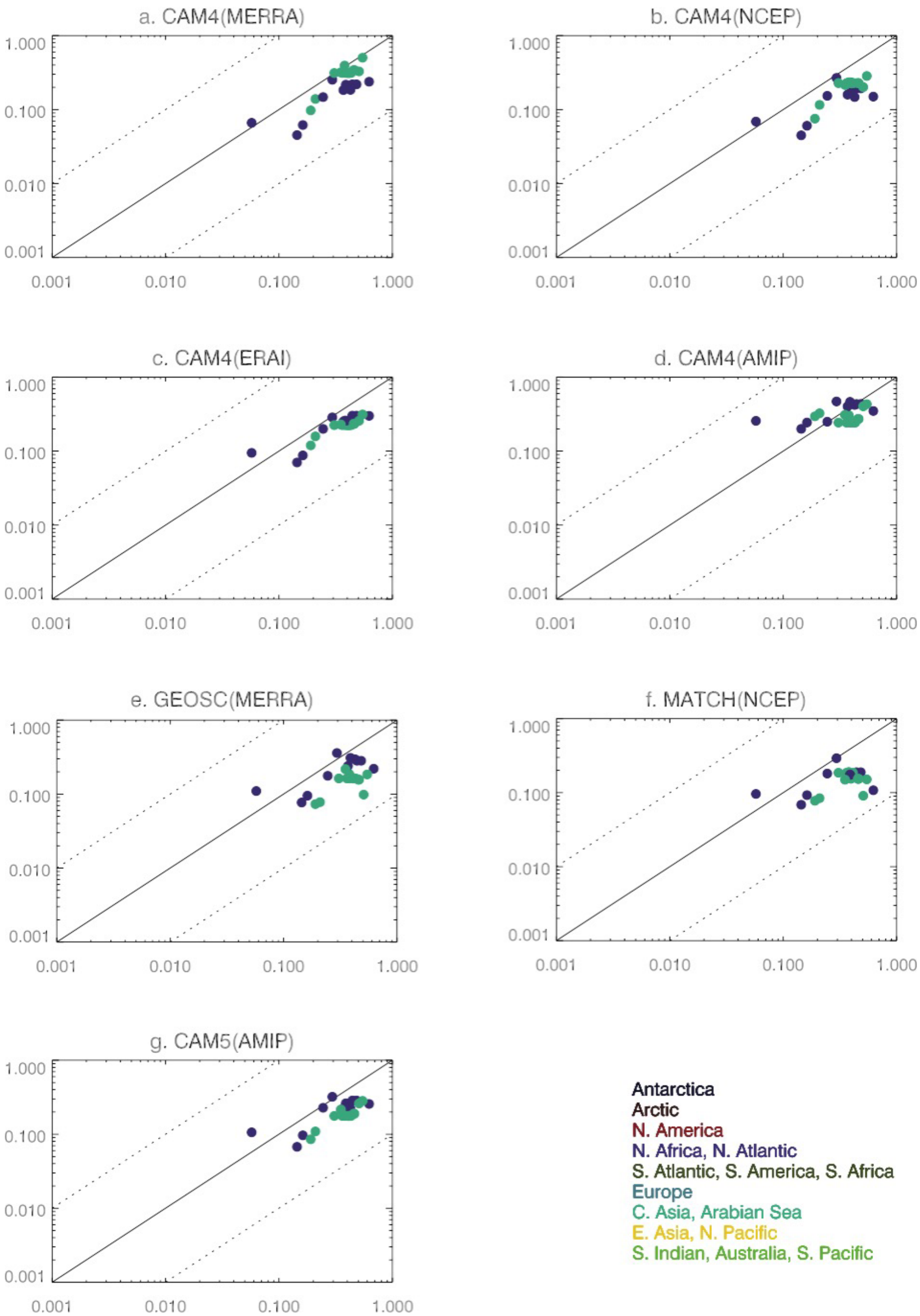

Figure S4: Scatterplot of annually averaged AOD measurements (shown in Figure S3) versus model results for the cases considered here: CAM4 (MERRA) (a), CAM4 (NCEP) (b), CAM4 (ERAI) (c), CAM4 (AMIP) (d), GEOSC (MERRA) (e), MATCH (NCEP) (f), CAM5 (AMIP) (g). Correlation coefficients for these comparisons are shown in Table 2. Colors indicate broad regions as in legend.

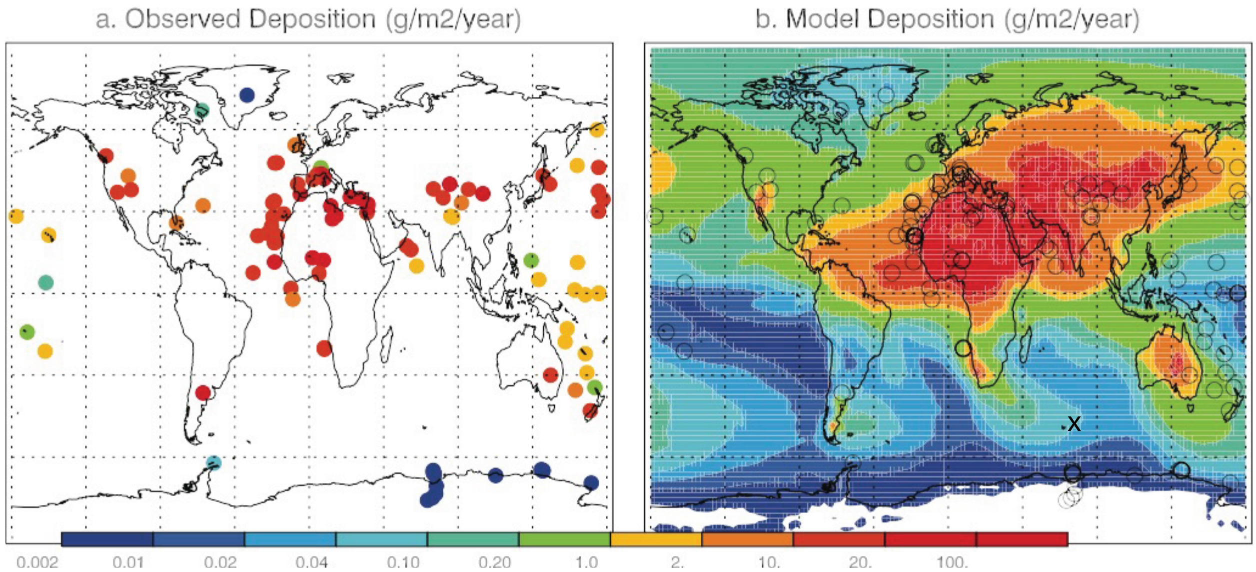

Figure S5: Spatial plot of the observed annually average deposition in dust dominated regions (a) and model simulation using CAM4 (MERRA) case (b). Observational synthesis from (Albani *et al.*, 2014). Observational sites used in the correlation coefficient comparison to shown with circles, while the ‘x’ mark the long-term stations used for IAV evaluation.

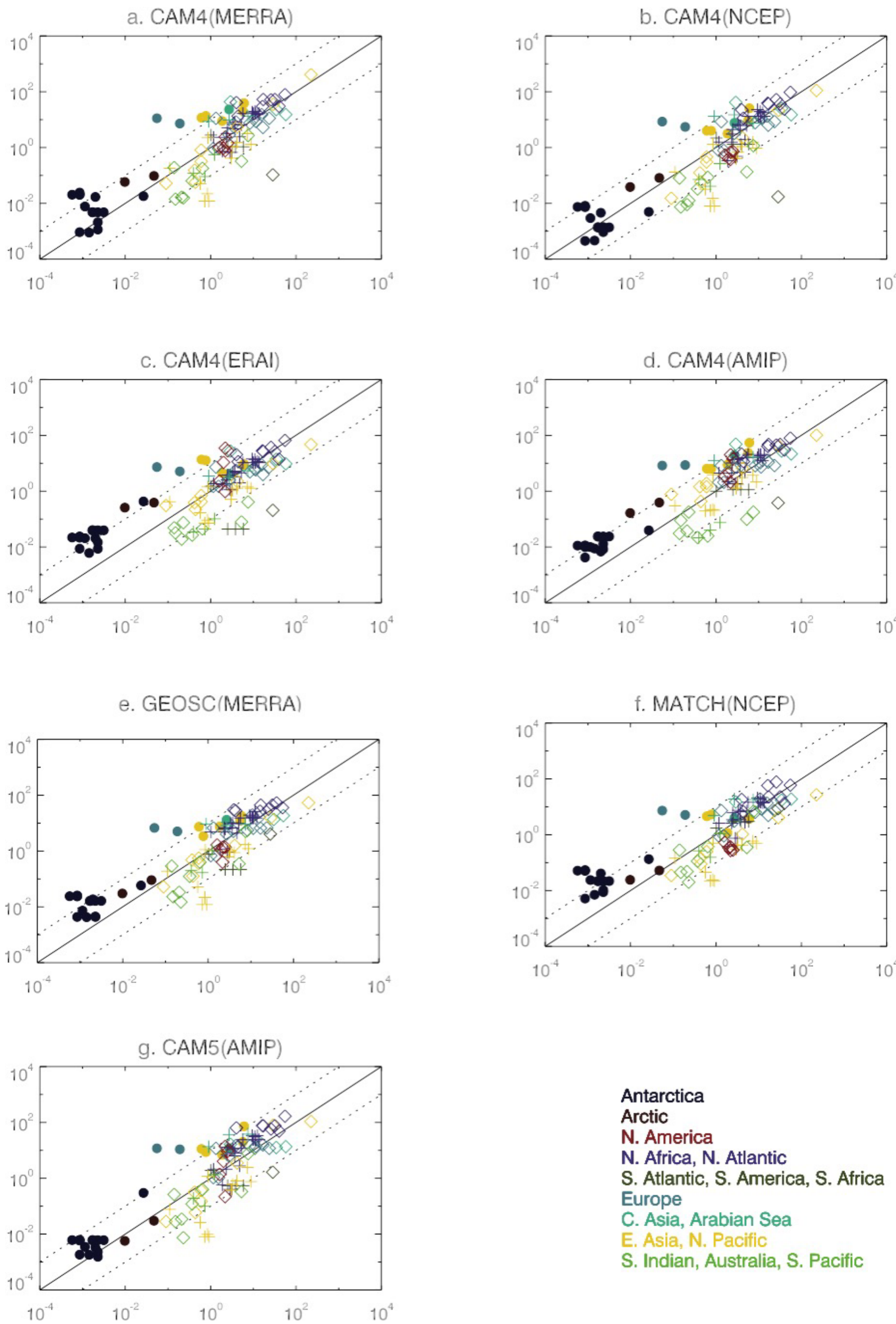

Figure S6: Scatterplot of annually averaged deposition measurements (shown in Figure S5) versus model results for the cases considered: CAM4 (MERRA) (a), CAM4 (NCEP) (b), CAM4 (ERAI) (c), CAM4 (AMIP) (d), GEOSC (MERRA) (e), MATCH (NCEP) (f), CAM5 (AMIP) (g). Correlation coefficients for these comparisons are shown in Table 2. (Circles=ice cores; diamonds=terrestrial deposits; crosses=marine sediments). Colors indicate broad regions as in legend.

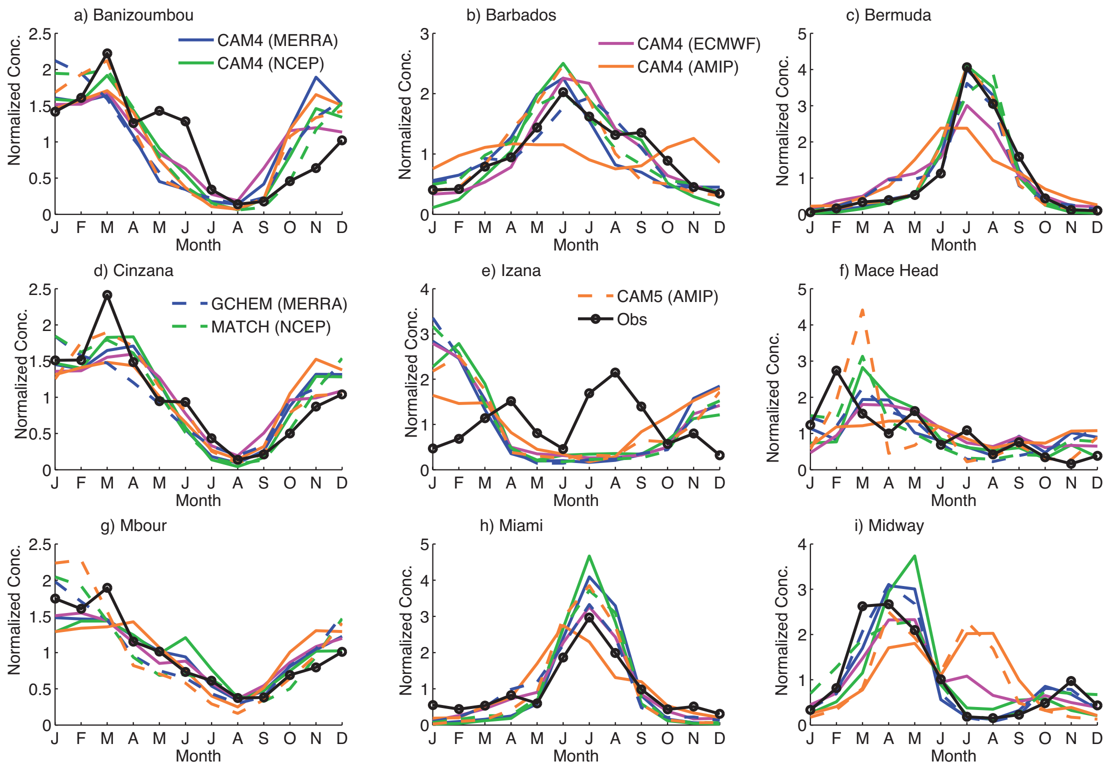

Figure S7: Climatological monthly average time series of dust concentration divided by the mean of each time series (unitless) at stations a) Banizoumbou, b) Barbados, c) Bermuda, d) Cinzana, e) Izana, f) Macehead, g) Mbour, h) Miami, i) Midway. Observations are in black and are from the locations and citations in Table 2. Different colors and line styles indicate the different model versions: CAM4 (MERRA) (blue solid), CAM4 (NCEP) (green solid), CAM4 (ERAI) (pink solid), CAM4 (AMIP) (orange solid), GCHEM (MERRA) (blue dashed), MATCH (NCEP) (green dashed), CAM5 (AMIP) (orange dashed). The monthly means are divided by the long term annual mean to allow comparison with interannual variability, since they are similarly normalized (Figure 1).

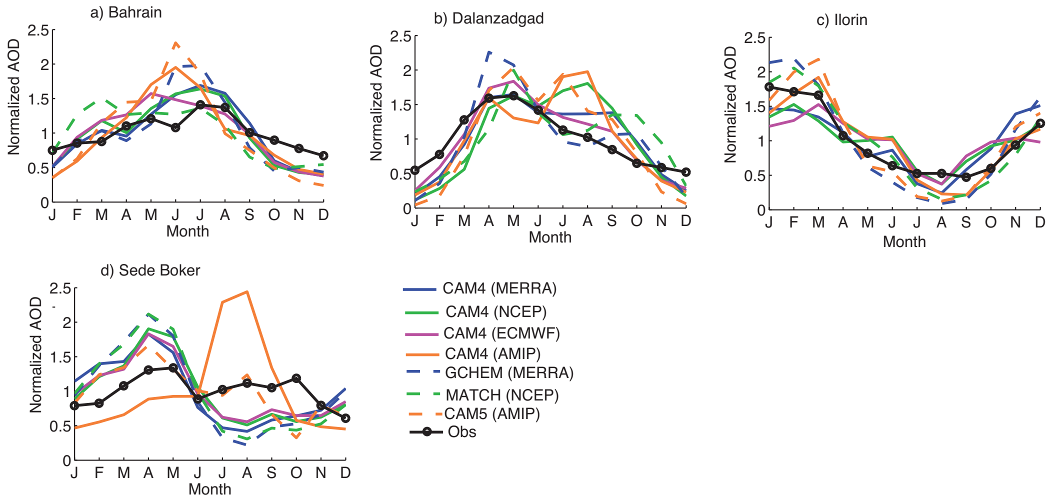

Figure S8: Climatological monthly average aerosol optical depth (AOD) for model simulations (based on dust only), compared with AERONET observations for: a) Bahrain b) Dalanzadgad, c) Ilorin and d) Sede Boker for each of the different model versions (Colors and information are the same as in Figure 1, but for the AOD). Observational data from AERONET stations (citations and locations listed in Table 2). The monthly means are divided by the long term annual mean to allow comparison with interannual variability, since they are similarly normalized (Figure 2).

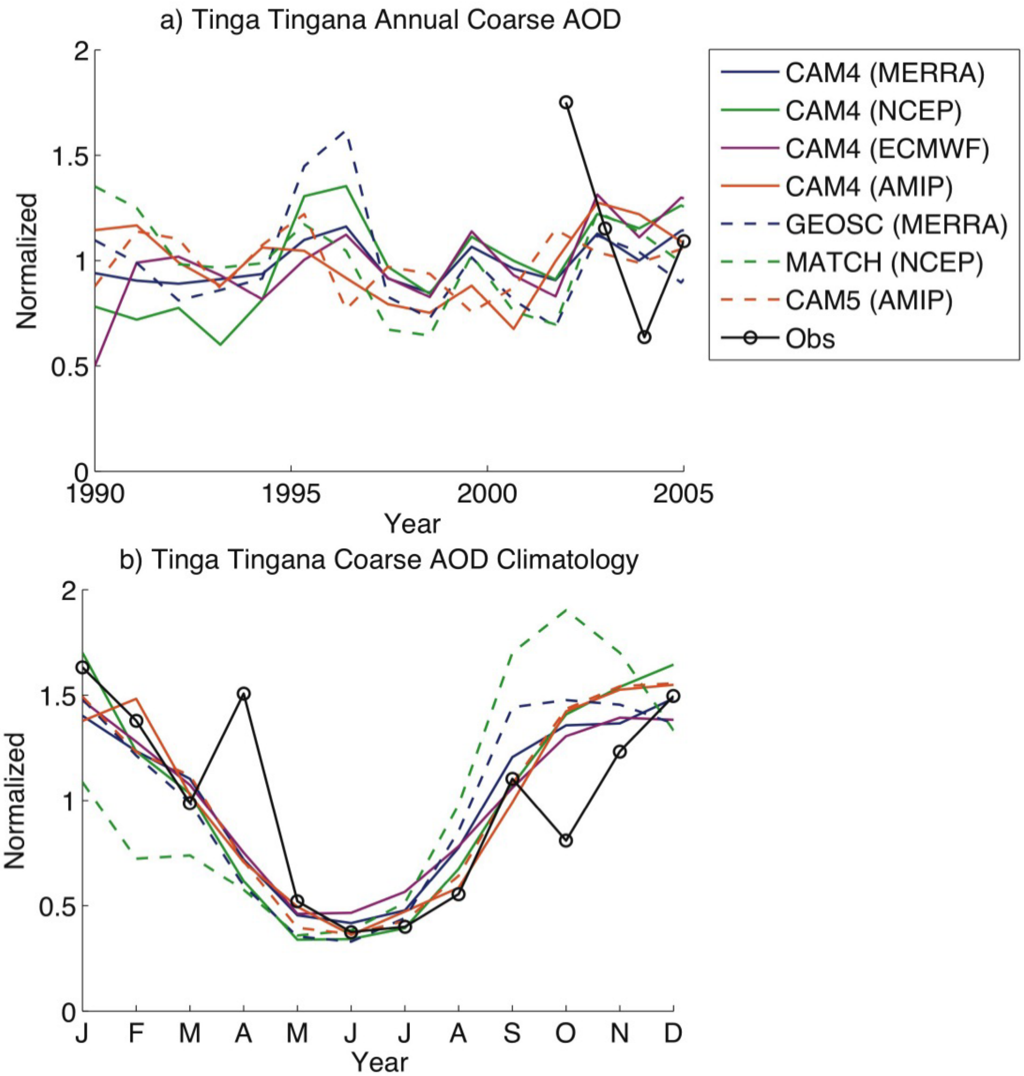

Figure S9: Timeseries of (a) annual mean AOD and (b) mean seasonal cycle for model simulations (based on dust only), compared with AERONET observations Tinga Tingana (28.9758°S, 139.9908°E) coarse mode aerosols.

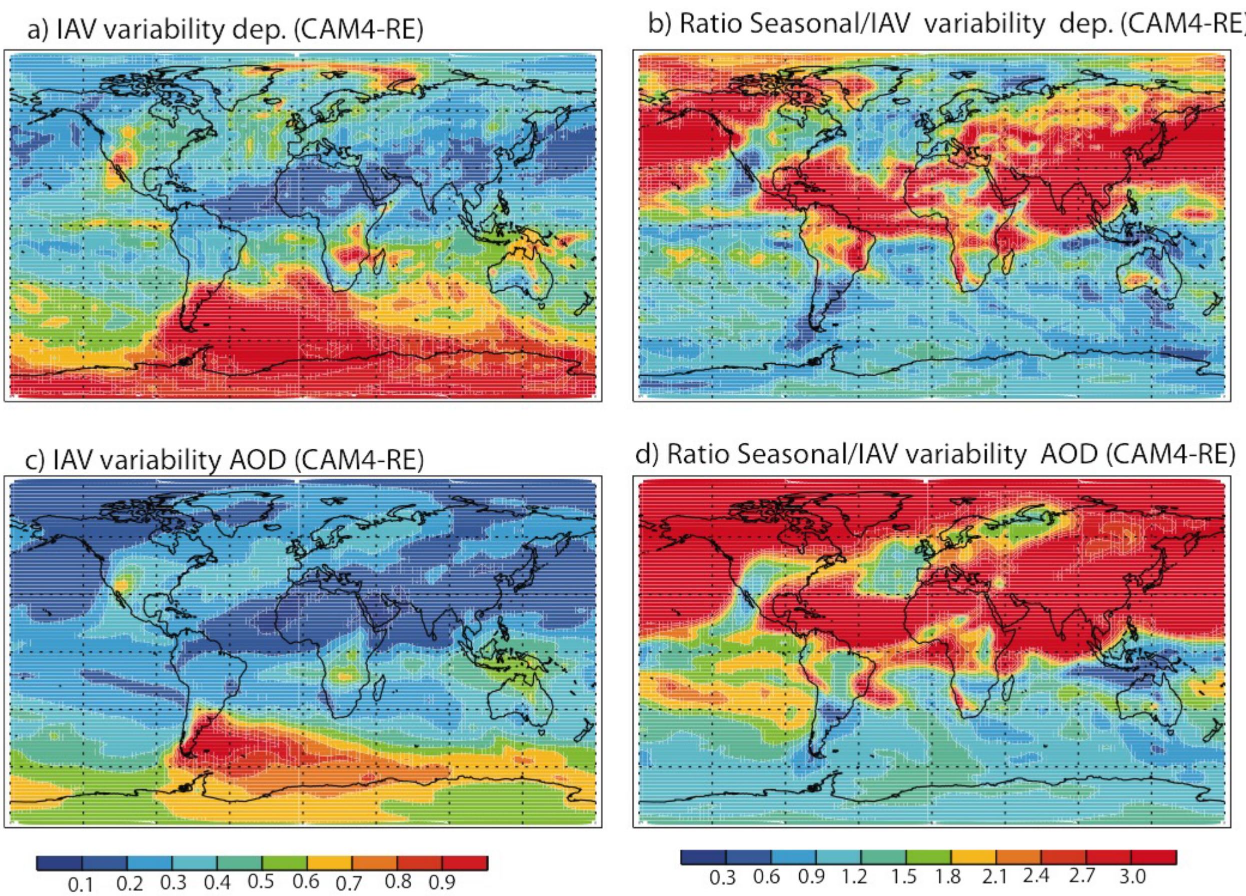

Figure S10: Spatial plot of the modelled IAV variability in the model simulations at each grid box (CAM4-RE is the mean of CAM4 (MERRA), CAM4 (NCEP) and CAM4 (ERAI)), where variability is unitless and is the standard deviation divided by the mean of the annual mean between 1990 and 2005 for a) deposition and c) AOD. The ratio of the seasonal variability over the IAV variability (calculated using the 12 climatological monthly means) is shown in the right hand panel for b) deposition and d) AOD. Same as Figure 6a and 6b but for different variables.

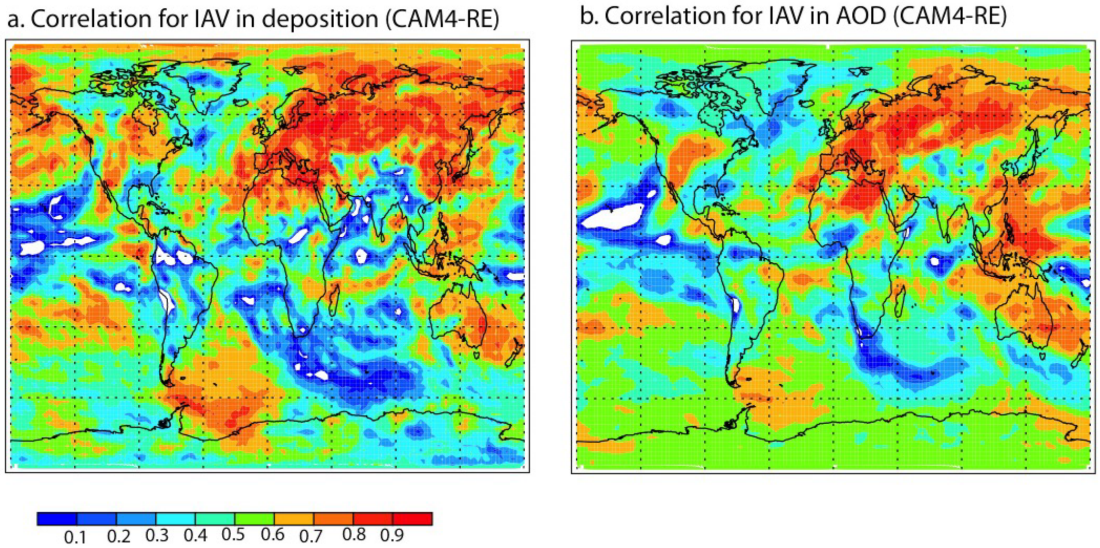

Figure S11: Spatial plot of the average temporal rank correlation of the annual mean modelled values. The correlation is calculated between the CAM4-Reanalysis models (CAM4 (MERRA); CAM4 (NCEP) and CAM4 (ERAI) and averaged; left hand column (a and c) and the models driven by the same meteorology (average of CAM4 (MERRA) vs. GCHEM (MERRA) and CAM4 (NCEP) vs. MATCH (NDEP) (b and d) for deposition (a and b) and AOD (c and d). Same as Figure 7 but for different variables.

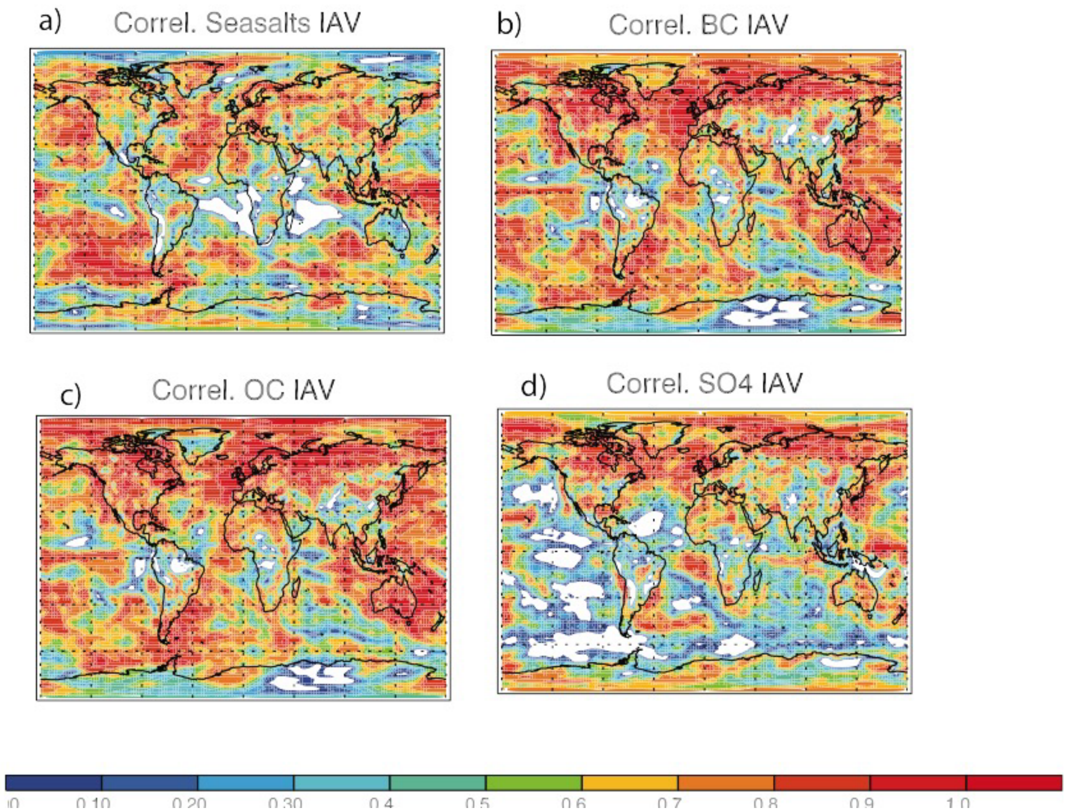

Figure S12: Correlation maps for the CAM4 (MERRA) and CAM4 (NCEP) simulations for additional aerosol species (Sea salts (a), black carbon (BC) (b), organic carbon (OC) (c), and sulfate (SO4) (c), for annual means (interannual variability).

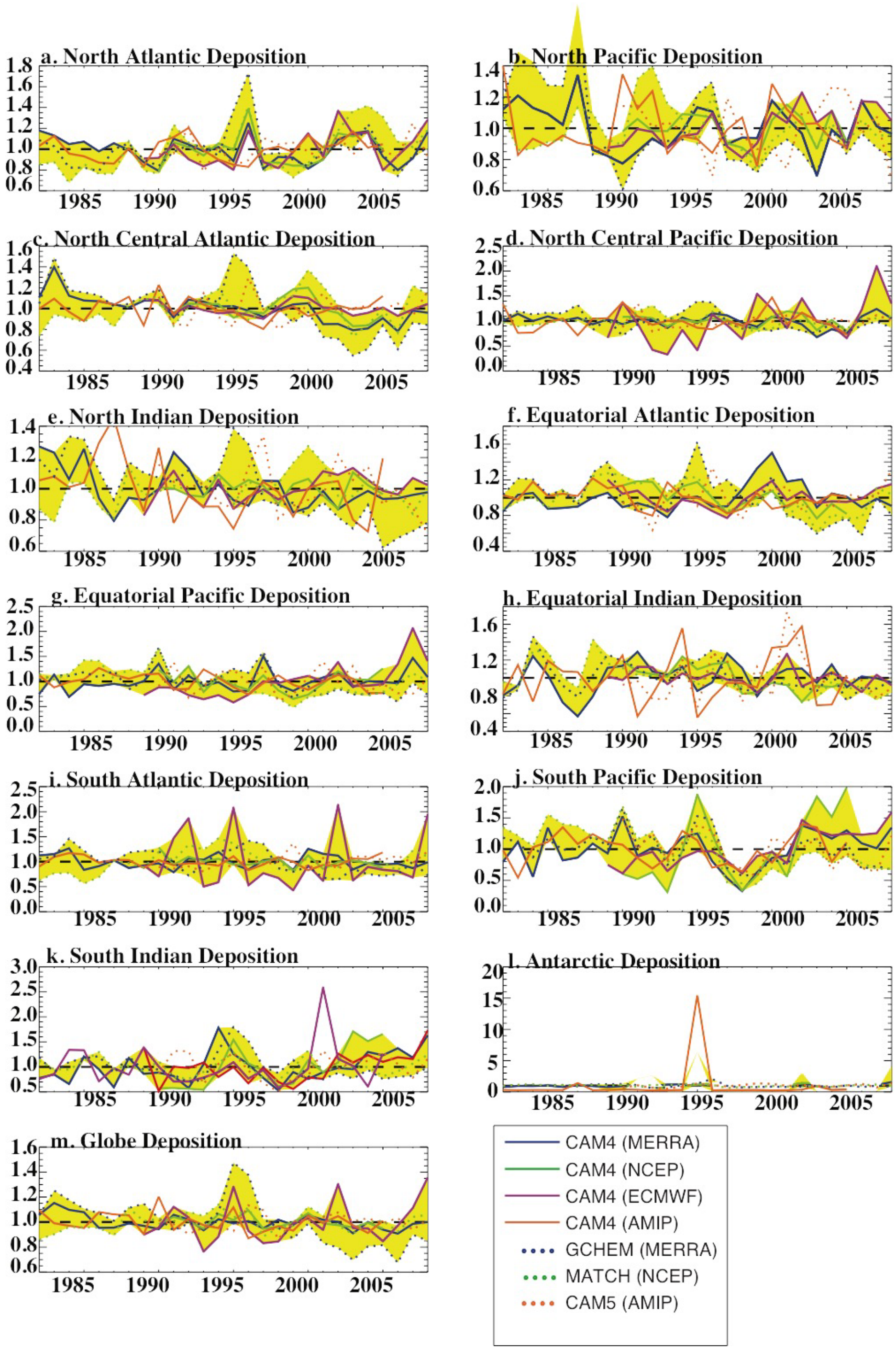

Figure S13: Time series of the annual mean deposition flux in different ocean regions as simulated in the different model versions (different colors, as in legend). All time series are normalized by the climatological mean in order to focus on interannual variability (shown in Table S9). The yellow highlighted area is the area encompassed by the 5 reanalysis-based simulations (CAM4 (MERRA), CAM4 (NCEP), CAM4 (ERAI), GCHEM (MERRA), MATCH (NCEP)). The ocean basin areas are defined as over ocean in the regions in Table S8 from (Gregg et al., 2003).

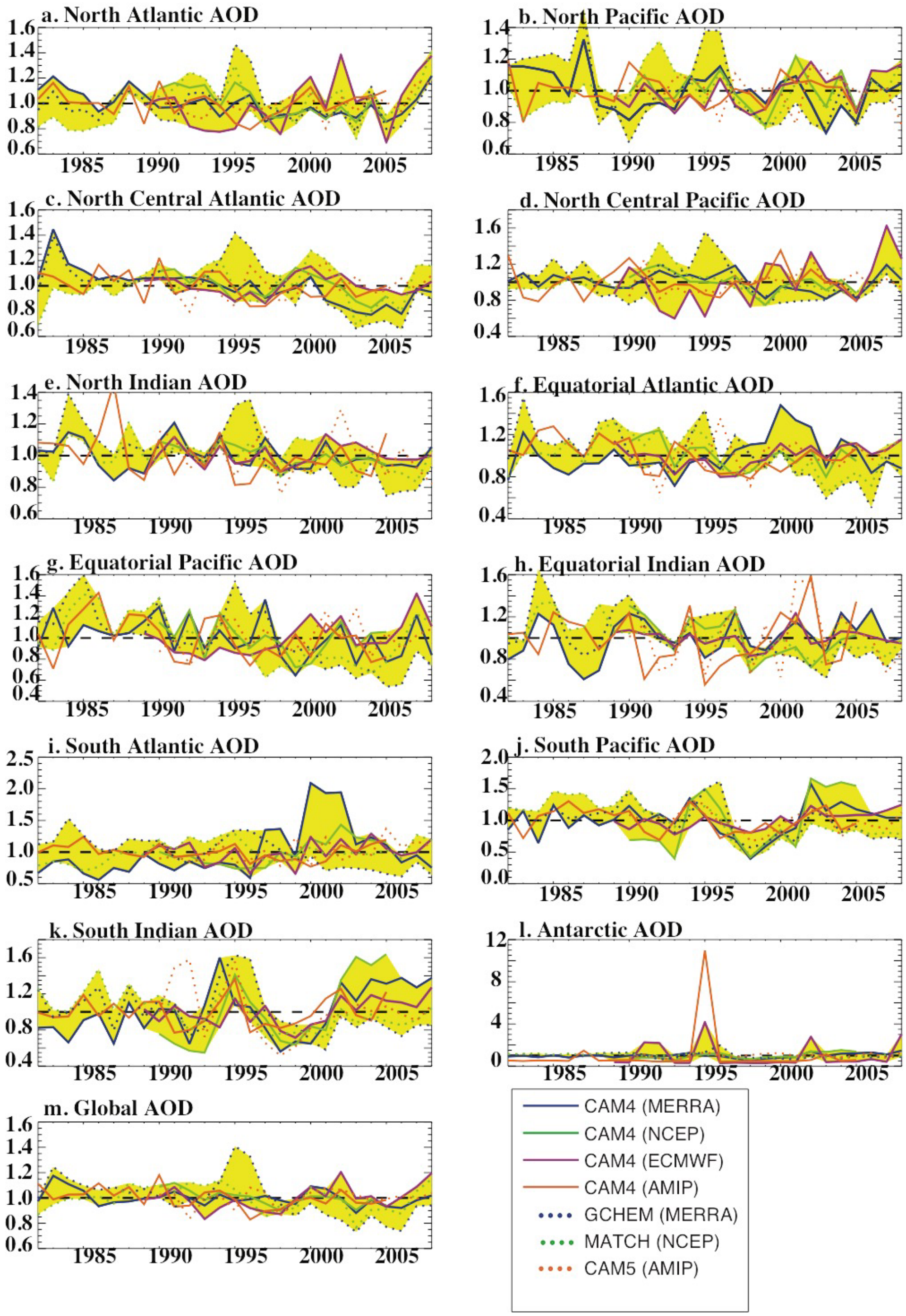

Figure S14: Time series of the annual mean Aerosol Optical Depth (AOD) in different ocean regions as simulated in the different model versions (different colors, as in legend). All time series are normalized by the climatological mean (Table S10) in order to focus on interannual variability. The yellow highlighted area is the area encompassed by the 5 reanalysis-based simulations (CAM4 (MERRA), CAM4 (NCEP), CAM4 (ERAI), GCHEM (MERRA), MATCH (NCEP)). The ocean basin areas are defined as over ocean in the regions in Table S8 from (Gregg et al., 2003).

Albani S, Mahowald N, Perry A, Scanza R, Zender C, Flanner MG (2014) Improved representation of dust size and optics in the CESM. Journal of Advances in Modeling of Earth Systems*,* **6**, doi:10.1002/2013MS000279.
Holben BN, Tanre D, Smirnov A *et al.* (2001) An emerging ground-based aerosol climatology:Aerosol optical depth from AERONET. Journal of Geophysical Research*,* **106**, 12067-12097.